Macromolecules

Article

pubs.acs.org/Macromolecules

Advanced Polymerization and Properties of Biobased High T_g polyester of Isosorbide and 1,4-Cyclohexanedicarboxylic Acid through *in Situ* Acetylation

Won Jae Yoon,[†] Kwang Sei Oh,[‡] Jun Mo Koo,[†] Jong Ryang Kim,[‡] Kee Jung Lee,[§] and Seung Soon Im*,[†]

[†]Department of Organic and Nano Engineering, College of Engineering, Hanyang University, 17 Haengdang-dong, Seongdong-gu, Seoul, 133-791

[‡]SK Chemicals Co., Ltd., 686 Sampeoung-dong, Bundang-gu, Seongnam-si, Gyeonggi-do 463-400

[§]Department of Chemical Engineering, College of Engineering, Hanyang University, 17 Haengdang-dong, Seongdong-gu, Seoul, 133-791

Supporting Information

ABSTRACT: The synthetic problems associated with melt polymerizations to form homopolyesters of isosorbide (ISB) and rigid diacids could potentially be solved by using catalyst systems with acetic anhydride (Ac_2O). A catalyst consisting of dibutyltin oxide, germanium oxide, and Ac_2O exhibited excellent performance characteristics in syntheses of a high-molecular-weight homopolyester of ISB and *cis*/*trans*-1,4-cyclohexanedicarboxylic acid (CHDA), also referred to as poly(isosorbide *cis*/*trans*-1,4-cyclohexanedicarboxylate) (PICD). The acetylation of ISB using Ac_2O during esterification decreased the steric hindrance of ISB and accelerated the chain growth of PICD. Gel permeation chromatography data confirmed the formation of a high-molecular-weight PICD (71 100 weight-average molecular weight and 14 300 number-average molecular weight) using 0.02 mol of Ac_2O. The glass transition temperature of PICD was almost 131 °C at 0.02 mol of Ac_2O and decreased with increasing amounts of Ac_2O due to the breaking of the rigid ring of ISB at higher concentrations of Ac_2O. The structure of opened ring ISB was confirmed using two-dimensional nuclear magnetic resonance (NMR) and distortionless enhancement by polarization transfer NMR.

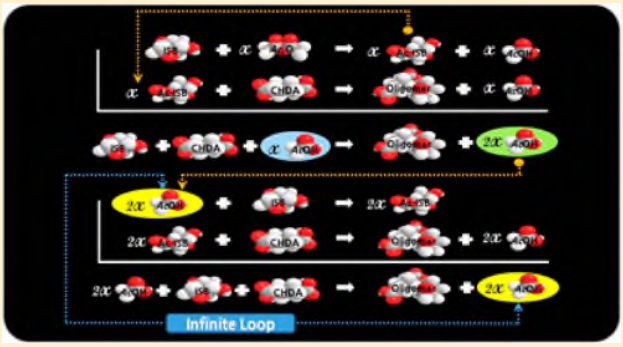

INTRODUCTION

1,4:3,6-Dianhydrohexitol, a biobased material that can be derived from biomass such as wheat, sugar, and corn, has been used in various polymer preparations, pharmaceuticals, and cosmetics.[1−6] It has three stereoisomers which are isosorbide (ISB), isomannide, and isoidide, respectively obtained from glucose, mannose, and fructose.[7,8] Among its three stereoisomers, ISB is the most easily accessible and affordable monomer for polymer synthesis[8,9] and is one of the most favorable candidates for renewable monomers used in addressing environmental issues and the depletion of petroleum resources.[10] When ISB is used as a monomer of polyester, the resulting polyester is not only environmentally desirable, but also has superior thermal and optical properties due to its molecular rigidity and the chirality of its asymmetrical hydroxyl groups. Several reports describe attempts to synthesize various polymers containing ISB, including polyesters,[11−24] polyurethanes,[25−29] epoxy,[30,31] polyamides,[32,33] polycarbonates, and liquid crystalline polymers.[34−38]

In homopolyesters made with ISB, the incorporation of terephthalic acid (TPA), an aromatic diacid, results in materials with high thermal stability and desirable mechanical properties. However, the formation of a homogeneous system during polymerization is problematic because both TPA and ISB are solid powders and TPA does not dissolve in ISB melts.[13] Furthermore, the low reactivity and volatility of ISB make it difficult to obtain a high-molecular weight polymer. Previous studies by Quintana et al.[10] describe syntheses of polyterephthalates from ethylene glycol (EG), 1,4-cyclohexanedimethanol (CHDM), and ISB. They reported the number-average molecular weights (M_n) and weight-average molecular weights (M_w) of PE(CIs)T terpolyester containing 15 mol % of CHDM and ISB of only 13 400 and 25 900 g mol^{-1}, respectively. A disadvantage of using TPA in a melt polymerization is that the molecular weight obtainable with ISB is low.[8] The fraction of unreacted terephthalic acid groups in PIT (homopolyester with TPA and ISB) is much higher than that in PET.[13]

Received: January 21, 2013
Revised: March 28, 2013
Published: April 3, 2013

 © 2013 American Chemical Society

ALIGN – EXHIBIT 2039
ClearCorrect Operating, LLC. v. Align Technology, Inc. IPR2025-00818

Scheme 1. Conformation of CHDA through a Twisted-Boat Intermediate

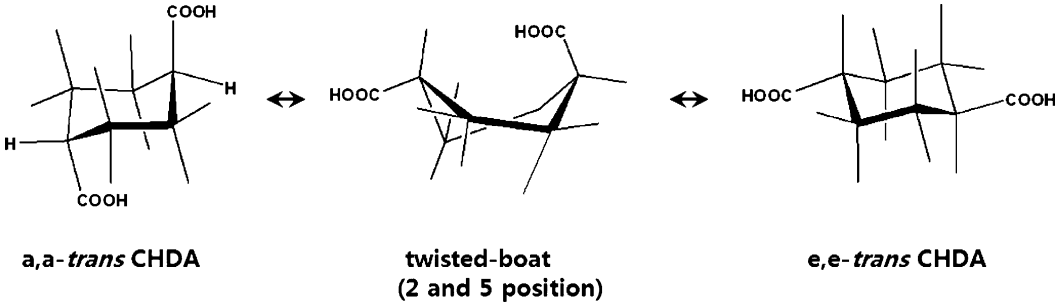

1,4-Cyclohexanedicarboxylic acid (CHDA), one of monomers used in the current study, has a lower melting point than TPA. The structure of CHDA is based on cyclohexane while the structure of TPA is based on a benzene ring. As a result, CHDA has better weatherability,[39] higher impact strength,[40] and faster stress relaxation.[41] CHDA has three isomers with chair conformations: axial, axial (a,a) *trans*-isomer, as well as an equatorial, equatorial (e,e) *trans*-isomer and an a,e *cis*-isomer. The transition between the *trans* conformations occurs through a twisted boat intermediate conformation. This results in high impact resistance and strong mechanical properties, as illustrated in Scheme 1.[40,41]

Noordover et al.[17,42] synthesized polyesters of succinic acid and ISB with titanium(IV) *n*-butoxide by melt polymerization and reported a final molecular weight of up to 2500 g mol^{-1}. This limitation is due to the low reactivity and intramolecular hydrogen bonding of the endohydroxyl group of ISB. Garaleh et al.[43] prepared homopolyesters of CHDA and ISB using three different methods. Of these, only the polycondensation of ISB and CHDA dichloride, which is more reactive than CHDA, yielded a M_n as high as 11 000 g mol^{-1}. This method, however, is not suitable for commercial polyester manufacture and it is not environmentally friendly.

A successful approach for improving the reactivity of ISB was to substitute an acetyl group at the end of the monomer and polymer chain during polymerization. Acetylation of ISB with acetic anhydride (Ac_2O) substantially accelerates chain growth during polymerization. In addition, a small amount of Ac_2O (2 mol % to ISB) drastically increases the molecular weight of ISB homopolyesters, much like a catalyst. This *in situ* acetylation method also activates the epimerization of CHDA toward a higher *trans* ratio from 22 mol % to 66 mol % at thermal equilibrium. The current report explores the cause of this epimerization and characterizes the thermal properties of PICD polymer. A proposed mechanism for PICD homopolyester polymerization by Ac_2O is also provided.

■ EXPERIMENTAL SECTION

Materials. CHDA (99.8%) with 22 mol % *trans*-isomer and ISB (99.8%, Roquette Freres S.A.) were supplied by SK Chemicals. The monomers were high-purity commercial products and used as received. Solvents and chemical reagents used for acetylation and characterization, including Ac_2O, AcOH, chloroform, *o*-chlorophenol, dichloromethane, and sodium bicarbonate, were all high-purity grade and used as received.

Synthesis of Polyesters. PICD was prepared using a 3-L bench reactor with a jacketed stainless steel vessel. The reactor was fitted with an anchor agitator, condenser, and a trap and was used for the esterification reaction. CHDA (1220 g, 7.09 mol), ISB (1040.8 g, 7.12 mol), germanium dioxide (200 ppm) and dibutyl tin oxide (150 ppm) were weighed into the reactor in a molar ratio of CHDA/ISB = 1/1.003. Ac_2O was added to the reactor at levels of 0−75 mol % relative to the level of ISB. After flushing three times with nitrogen to remove oxygen from the reactor, the reaction mixture was heated at 120 °C under 1 bar of nitrogen. After 1 h, the temperature was raised to 250 °C at rate of 100 °C per hour and held at 250 °C for an additional 2 h to reach the end point of esterification. Most of the H_2O and AcOH generated during the esterification reaction were distilled out at this stage. A sample of oligomer was carefully removed from the esterification reactor for analysis prior to polycondensation. The polycondensation reaction was performed in a different reactor fitted with a spiral agitator. The oligomer was transported from the esterification reactor to the polycondensation reactor through preheated pipeline at 250 °C. The temperature was then slowly increased to 265 °C while stirring at 98 rpm. The stirring speed was slowly decreased to 30 rpm with increasing degree of polymerization and the vacuum was reduced gradually to 0.4 mbar. Polycondensation was performed under isothermal conditions until the torque measured by the stirrer reached 2 N m. Finally, the pressure was returned to atmospheric pressure using nitrogen to prevent degradation by oxidation. The resulting polyester was removed from the reactor, quenched in a water bath, and analyzed.

Epimerization Test. *Acetylation of CHDA and Heat Treatment.* CHDA (50 g) was reacted with 65.2 g (2.2 mol) of Ac_2O in a nitrogen atmosphere in a 250-mL flask with a reflux system and a magnetic stir bar. The flask was heated gradually from room temperature to 120 °C and the mixture was stirred for 1 h in a closed system. The reacted mixture was removed from the flask and any remaining Ac_2O and AcOH were extracted using an evaporator under reduced pressure at 100 °C for 1 h.

Acetylated CHDA (Ac-CHDA) was divided into six different 50-mL flasks for heat treatment. Each flask was filled with 10 mL of Ac-CHDA and a magnetic stir bar. The Ac-CHDA was stirred for 1 h in a closed system at various temperatures between 200 and 250 °C.

Characterizations. *Intrinsic Viscosity.* The intrinsic viscosities of the polymers were measured using an automated Ubbelohde viscometer at 25 °C. Polymer samples (0.36 g) were carefully weighed and dissolved in 30 mL of *o*-chlorophenol. This solution was heated at 150 °C for 15 min and stirred with a magnetic stir bar to ensure complete dissolution. Each solution was then cooled to room temperature. Intrinsic viscosity values were calculated from relative viscosities.

Size Exclusion Chromatography (SEC). The M_n and polydispersity (M_w/M_n) were determined by gel permeation chromatography (GPC) using two Shodex LF804 columns at 40 °C (mixed bed, maximum pore size 3000 Å) equipped with a Malvern TDA 305 refractive index detector. Thirty milligrams of sample was predissolved in 3 mL of *o*-chlorophenol at 150 °C for 15 min, and 9 mL of chloroform was added at room temperature. *o*-Chlorophenol/chloroform (1/3) was used as the mobile phase at a velocity of 0.7 mL min^{-1}. Sample solutions were filtered through polytetrafluoroethylene microporous membranes (Merck Millipore) with a pore size of 0.45 μm prior to injection. Narrow and broad linear polystyrene standards were used for universal calibration.

Nuclear Magnetic Resonance (NMR). ^1H NMR spectra were obtained on a JEOL Oxford 600 spectrometer operating at 600 MHz.

Scheme 2. Polymerization Step of PICD Using *in Situ* Acetylation

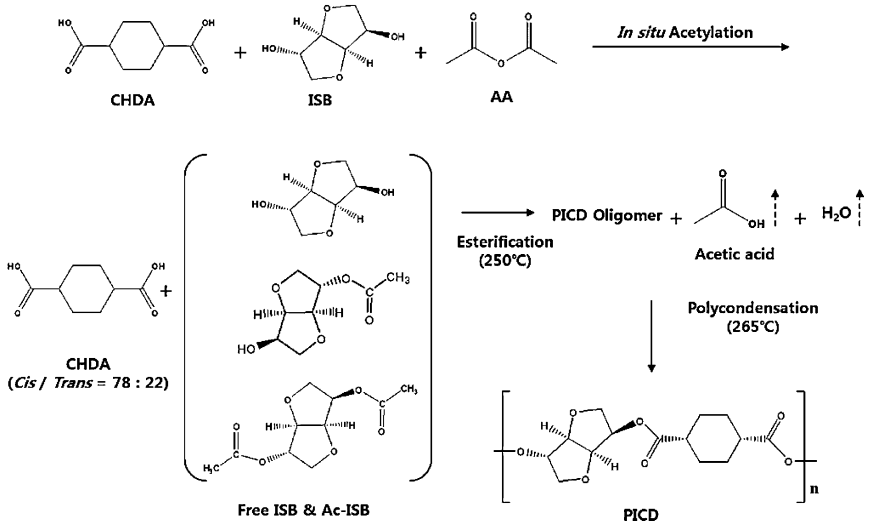

Deuterated chloroform was used as the solvent. Tetramethylsilane (TMS) was used as an internal standard and as a reference for chemical shift. Sixteen scans with 16K data points each were acquired for each ^{1}H NMR spectrum. Relaxation delays were 5 s. ^{13}C NMR spectra were recorded at 150 MHz using the same NMR spectrometer and solvent mixture. Each ^{13}C NMR spectrum was composed of 8192 scans with 64K data points each. Relaxation delays were 2 s.

Differential Scanning Calorimetry (DSC). DSC measurements were performed with a Mettler-Toledo DSC 820 calorimeter. Pellet samples of 8 ± 0.5 mg of PICD were enclosed in standard 40-μL aluminum cells. The samples were melted at 300 °C for 3 min, then quenched to 40 °C at a rate of 300 °C min^{-1}. The temperature was then raised at 10 °C min^{-1} from 40 to 300 °C in a nitrogen atmosphere. The glass transition temperature (T_g) was taken as the onset of the change in heat capacity associated with a transition.

■ RESULTS AND DISCUSSION

Synthesis and Proposed Mechanism. High-molecular-weight homopolyesters of CHDA and ISB have not been successfully synthesized through both melt and solution polymerization due to the low reactivity of ISB.[43] ISB is a V-shaped secondary diol having two fused rings at 120° to each other and two chemically nonequivalent hydroxyl groups.[8,10] The C5-OH is endo-oriented to form an intramolecular hydrogen bond with the oxygen atom of the adjacent tetrahydrofuran ring. The C5-OH is significantly less reactive than its exo-oriented counterpart, C2-OH.[9,44,45] This agrees with the results of Garaleh et al.[43] as described above. To change this steric environment, PICD homopolyesters were synthesized using CHDA and ISB through acetylation, substituting the hydroxyl end group with an acetyl group using Ac_2O. This was followed by esterification and polycondensation as illustrated in Scheme 2. The stoichiometric ratio between CHDA and ISB is near unity because of the low volatility of ISB at the reaction temperature, and the steric hindrance of the endo hydroxyl group of ISB is likely decreasing with acetylation. Ac_2O at concentrations of 0−75 mol %, relative to the levels of ISB, was added during the first stage of monomer esterification. The reactivity of ISB with Ac_2O is greater than that with CHDA. The electron-donating substituents of CHDA make its end groups less nucleophilic relative to the hydroxyl end groups of ISB. In accordance with this reasoning, the acetylation reaction with Ac_2O occurs primarily at the ISB subunits.

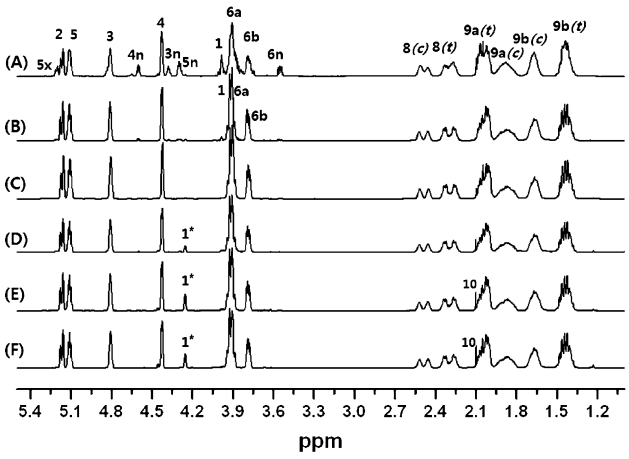

Figure 1. ^{1}H NMR spectra of PICD oligomer and polymers prepared with the various amounts of Ac_2O (a) ^{1}H NMR spectra of P M_w/M_n ICD oligomer, (b) PICD 2, (c) PICD 15, (d) PICD 30, (e) PICD 50, and (f) PICD 75, respectively.

The nucleophilicity of the hydroxyl oxygen atom in the endoposition of ISB is enhanced by intramolecular hydrogen bonding. This makes the endohydroxyl intrinsically more reactive than the exohydroxyl group.[46] However, higher steric hindrance occurs around the endohydroxyl group. Thus, the acetyl substitution may occur preferentially at the less reactive exohydroxyl. In this work, acetylation of ISB was conducted in an acidic environment, which lowered the effect of hydrogen bonding. Thus, ISB with a monoacetoxy end group was dominant in the exo position as shown Scheme 2. Tamion et al.[47] reported that by varying the parameters for the acetylation reaction (Ac_2O, 120−140 °C vs Ac_2O, PbO, room temp.), both monoesters can be prepared in yields of 70% and 80% for the exo and the endo positions, respectively. Noordover et al.[16,41] prepared polyesters from succinic acid and isosorbide in the presence of titanium(IV) *n*-butoxide. The ratio of terminal hydroxyl groups (endo/exo) was 6:4. This is confirmed in the ^{1}H NMR spectra in Figure 1(A), 5*n* and 5*x* (ratio of 5*n*/5*x* is

Table 1. Characteristics of PICD Synthesized with the Various Amount of Ac_2O

sample code[a]	Ac_2O contents (mol %)	IV[b] (°C)	M_n (g/mol)	M_w (g/mol)	M_w/M_n	*trans*-ratio (mol %)	T_g[e] (°C)
PICD-0	0	–	–	–	–	–	–
PICD-1	1	0.40	11 600	26 900	2.3	64.9	116
PICD-2	2	0.61	14 300	71 100	5.0	63.6	131
PICD-15	15	0.74	15 900	94 100	5.9	63.8	131
PICD-30	30	0.65	18 300	84 800	4.6	63.3	128
PICD-50	50	0.73	17 100	95 100	5.6	63.5	124
PICD-75	75	0.48	11 600	53 100	4.6	63.8	119

[a]Sample codes denote the mol % of Ac_2O added relative to ISB. [b]Intrinsic viscosity (dL g^{-1}) measured in *o*-chlorophenol at 30 °C. [c]Number-average molecular weight (M_n) and weight-average molecular weight (M_w) determined by GPC. [d]*Trans* mole fractions of CHDA isomers in the PICD polymers estimated by ^{1}H NMR. [e]Glass transition temperatures measured by DSC.

Scheme 3. Possible Structures of PICD polymer

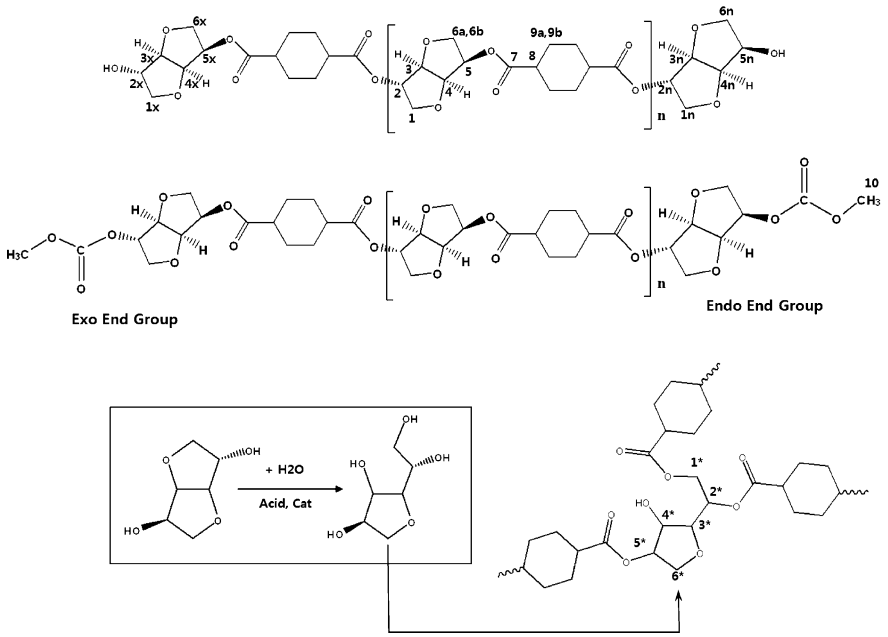

2:1), which indicate that the endohydroxyl group of ISB is dominant over the exo end group.

Table 1 summarizes the analytical results of various PICD samples as a function of Ac_2O content. The M_n of the samples tended to increase with Ac_2O contents up to 30−50 mol %. In contrast, the M_n of PICD-75 rapidly decreased, presumably due to the reverse reaction induced by the highly acidic atmosphere during polymerization. The values of M_w/M_n (MWD) of PICD-2−PICD-75 are very broad as compared to PICD-1. This phenomenon can be ascribed to the formation of branch structure by reverse reaction of ISB (this will be discussed later in detail).

The chemical structure and composition of PICD were examined by ^{1}H NMR spectra shown in Figure 1. Peak assignments were established by 2D NMR spectroscopy, which provided detailed information about the structure of PICD shown in Scheme 3. Various NMR techniques, including correlation spectroscopy (COSY), heteronuclear single-quantum correlation spectroscopy (HSQC), heteronuclear multiple-bond correlation spectroscopy (HMBC), and distortionless enhancement by polarization transfer (DEPT) were employed to determine the sequence of specific protons and carbon atoms in PICD-50. Peaks in the ^{1}H NMR spectrum of the ISB moiety at δ 3.95, δ 5.13, δ 4.45, δ 4.83, δ 5.18, δ 3.92, and δ 3.82 ppm were assigned to hydrogen atoms 1, 2, 3, 4, 5, 6a, and 6b, respectively. In the ^{1}H NMR spectrum of the CHDA moiety, two methine protons, H8, yielded peaks around 2.31 and 2.51 ppm, indicating the *trans*- and *cis*-isomers, respectively. Both peaks exhibit double splitting, owing to the fact that the end groups of ISB have different steric environments. The methylene protons, H9 of the *trans*-isomer, are identified by peaks at 1.45 and 2.07 ppm. The *cis*-isomer peaks were observed at 1.69 and 1.91 ppm. The ratio of *cis*- to *trans*-isomers in CHDA was determined by integration of the peaks corresponding to H8 (*c*) (2.51 ppm) and H8 (*t*) (2.31 ppm) (see Table 1). As shown in Figure 1, the peak at 4.27 ppm can be conspicuously observed in the NMR spectrum at levels of Ac_2O above 30 mol % (PICD 30). The peak increases with increasing Ac_2O content. This peak also increases with acidity as the result of a reverse reaction (hydrolysis) with ISB. This effect will be discussed in greater detail below.

Using COSY spectra (Figure 2) it was possible to follow the presence of ISB residues bonded at both sides to CHDA (Scheme 3). The presence of ISB fragments was confirmed by correlation signals 1/2, 3/4, 4/5, 5/6a, 5/6b, and 6a/6b in Figure 2. However, because of the V-shaped structure of ISB and its two five-membered rings, correlation signals 2/3 were not detected in the COSY spectrum. On the basis of these

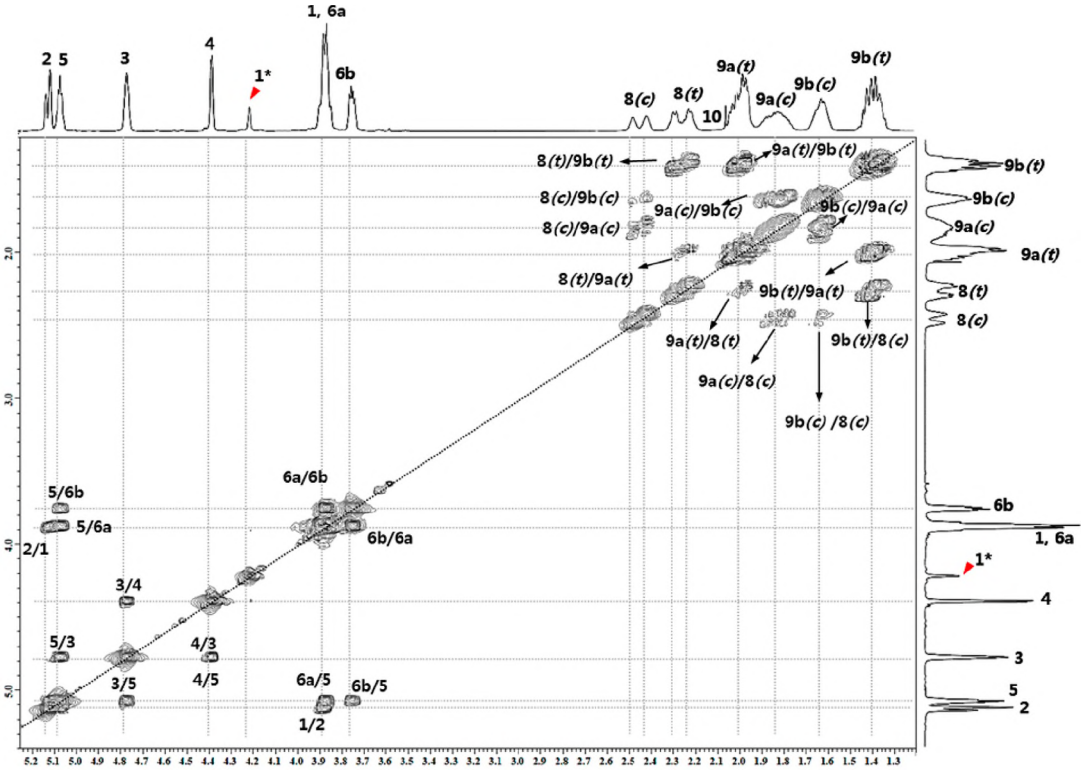

Figure 2. Correlation spectrum (COSY) of PICD 50.

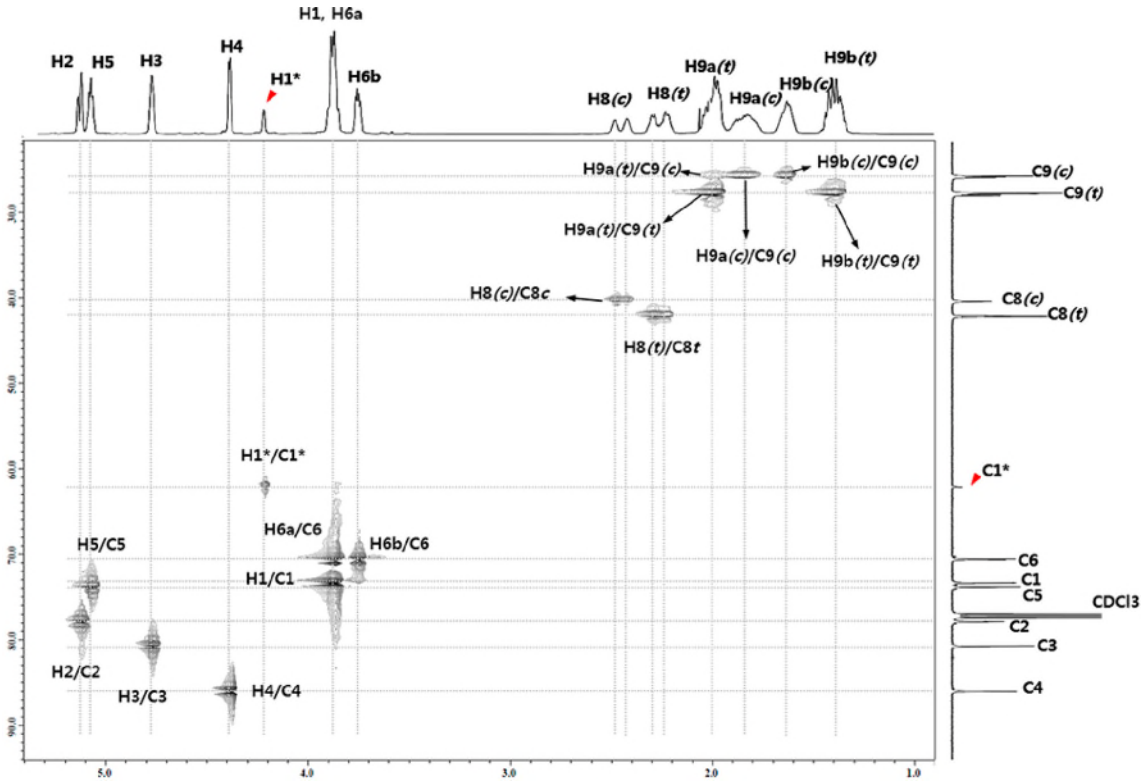

Figure 3. Heteronuclear single-quantum correlation spectrum (HSQC) of PICD 50.

results, proton signals were then assigned to the corresponding ^{13}C signals in the HSQC spectrum shown in Figure 3. The peaks in the ^{13}C NMR spectra of PICD 50 at δ 73.3, δ 77.3, δ 80.7, δ 86.0, δ 73.8, δ 70.6, δ 174.4, δ 40.3, δ 42.2, δ 25.8, and δ 28.0 ppm were assigned to 1, 2, 3, 4, 5, 6, 7, 8 *cis* (C8(*c*)), 8 *trans* (C8(*t*)), 9 *cis* (C9(*c*)), and 9 *trans* (C9(*t*)) carbon atoms,

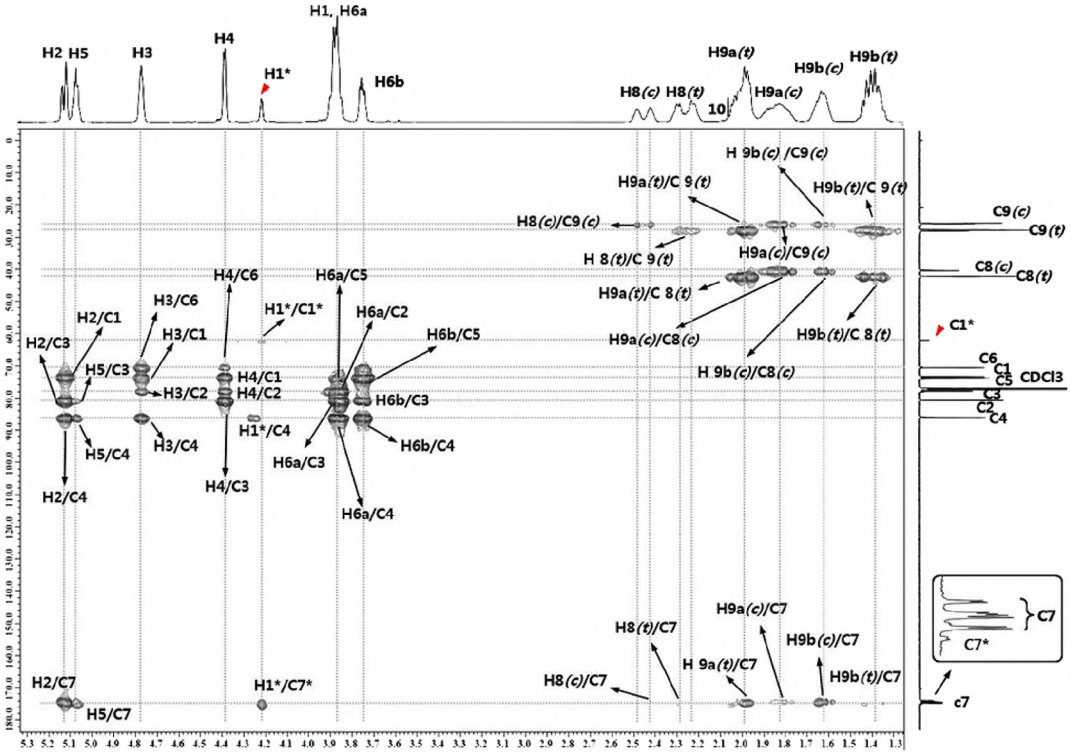

Figure 4. Heteronuclear multiple-bond correlation spectrum (HMBC) of PICD 50.

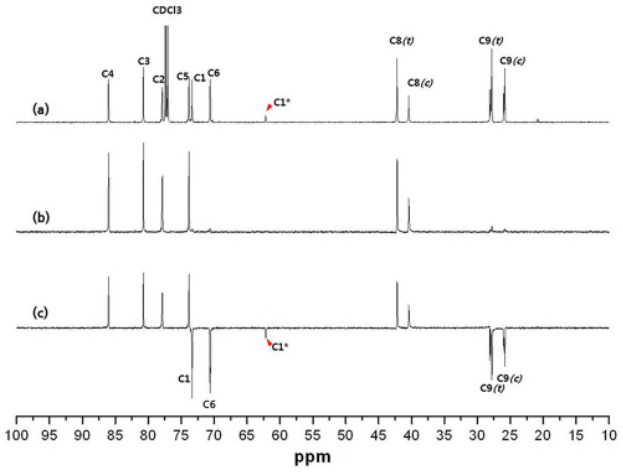

Figure 5. Distortionless enhanced by polarization transfer spectrum (DEPT) of PICD 50 (a) ^{13}C NMR spectra of PICD-50, (b) DEPT(90 angle) of PICD-50, and (c) DEPT (135 angle) of PICD-50.

respectively. These assignments were confirmed by correlation signals H1/C1, H2/C2, H3/C3, H4/C4, H5/C5, H6a/C6, H6b/C6, H8(*c*)/C8(*c*), H8(*t*)/C8(*t*), H9a(*t*)/C9(*c*), H9a(*t*)/C9(*t*), H9a(*c*)/C9(*c*), H9b(*c*)/C9(*c*), and H9b(*c*)/C9(*t*) at 3.95/73.3, 5.13/77.3, 4.45/80.7, 4.83/86.0, 5.18/73.8, 3.92/70.6, 3.82/70.6, 2.51/40.3, 2.31/42.2, 1.45/25.8, 1.45/28.0, 1.69/25.8, 1.91/25.8, and 1.91/28.0 ppm, respectively, in the HSQC spectrum.

ISB is formed by the dehydration of 1,4-sorbitan, an intermediate between ISB and sorbitol, under acidic conditions with a catalyst. Thus, hydration of ISB occurs if the Ac_2O content is high enough during polymerization, forming a branched structure as shown in Scheme 3. In numerous NMR peak assigning programs, the 1* hydrogen of the branched structure of the open-ring ISB moiety appears at around 4.2 ppm in the ^{1}H NMR spectrum. This structure was confirmed with DEPT and HMBC. In Figure 4, analysis of the HMBC spectrum shows correlation signals between H1*/C7* and H1*/C1* (Scheme 3) at 4.27/174.8 and 4.27/62.2 ppm, respectively. Additional evidence for the presence of C1* in open-ring ISB is given in Figure 5. DEPT at an angle of 135° yields all methane and methyl carbon atoms in a phase opposite that of a methylene carbon atom. The C1* peak (62.2 ppm) is a methylene carbon atom because it yields a negative signal as shown in Figure 5C. The H1* and C1* signals likely originate from the open-ring ISB.

In this experiment, the relative amount of *trans* configurations of the CHDA isomer dramatically increased, regardless of Ac_2O content, from 22 mol % to around 66 mol % (thermal equilibrium) after polymerization.

The *trans* ratio of CHDA changes only slightly during the melt polymerization. Colonna et al.[48] reported on the parameters affecting the polymerization and *cis*/*trans* isomerization of PCCD, which is a homopolyester made from CHDA and 1,4-cyclohexane dimethanol (CHDM). They stated that isomerization of CHDA occurs only slightly toward the thermodynamically stable *trans* ratio (66 mol %) during polymerization. The degree of change in the *trans* ratio was as follows: (1) The ratio of the *trans*-isomer of CHDA changes from 99 to 91 mol % during polymerization at 250 °C, (2) a *trans* ratio of 22 mol % increases to 29 mol % at 250 °C, and (3) a *trans* ratio of 99 mol % decreases to 91, 88, and 85 mol % at polymerization temperatures of 240, 250, and 260 °C, respectively.

As shown in Table 1S (see the Supporting Information), all of the PICD oligomers and polymers exhibited *trans* ratios

Scheme 4. Proposed Mechanism of Acidolysis and Epimerization of PICD Esterification Reaction

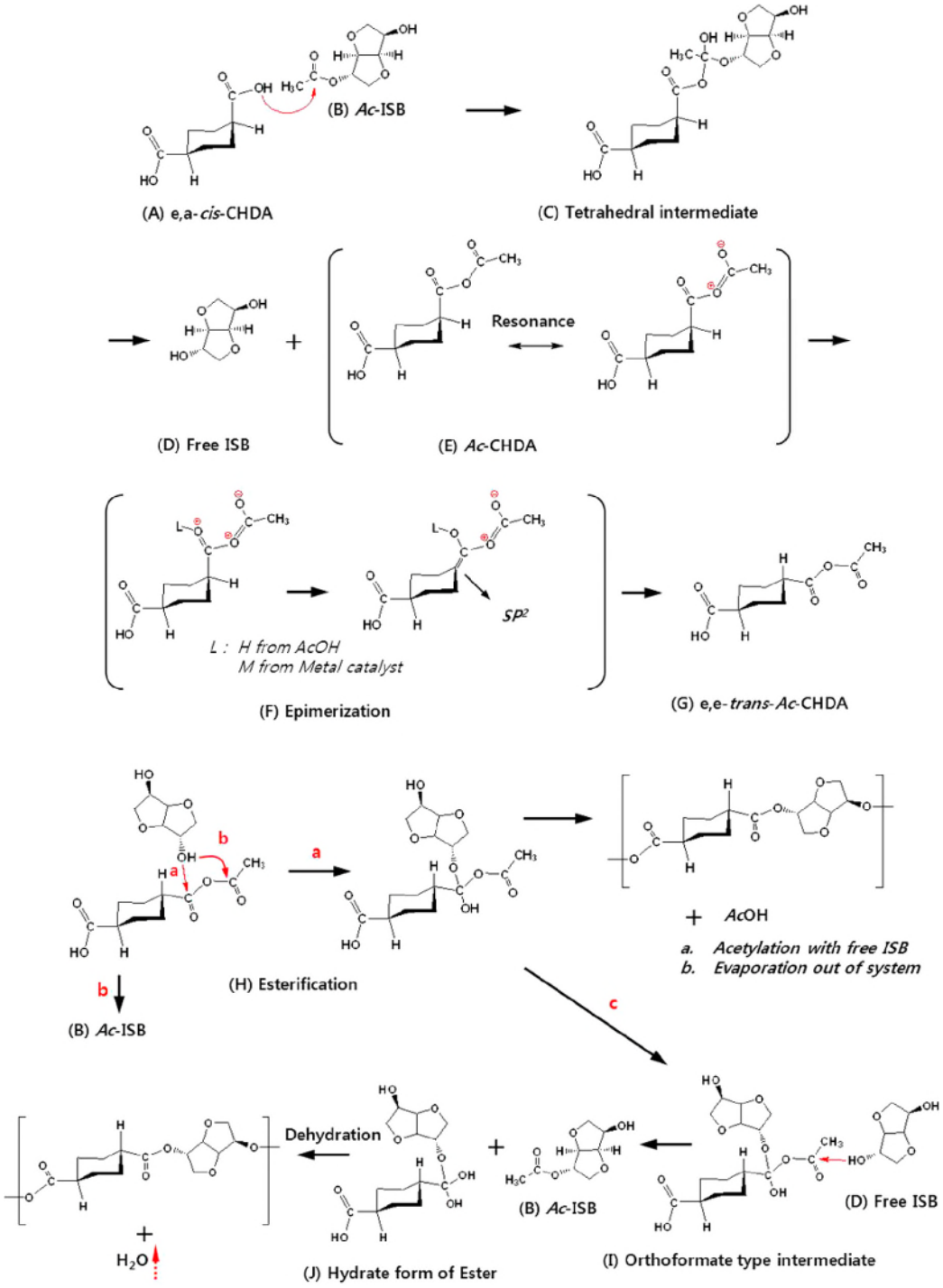

above 60 mol % regardless of the concentration of Ac_2O. Epimerization seemed to be activated by an increase in the acidity of the system. However, this explanation is insufficient to explain the results obtained with PICD-1 or PICD-2, which had extremely low amounts of Ac_2O. These phenomena can be explained by the proposed mechanism in Scheme 4. First, a hydroxyl group of e,a *cis*-CHDA (A) attacks the carbonyl carbon atom of Ac-ISB (B), generating a tetrahedral intermediate (C). The resonance stabilized Ac-CHDA (E) is more easily enolized than free CHDA and enol-keto tautomerization occurs, yielding the more stable e,e *trans-Ac*-CHDA. During epimerization (F), as the carbonyl changes back to its original structure, the planar sp^2 hybridized carbon atom eliminates stereoselectivity. The proton reverts to the axial position, which is more thermodynamically stable. This leads to the formation of the more stable e,e *trans*-CHDA (G). Hence, the epimerization of Ac-CHDA can occur at lower temperatures than that of free CHDA. In the esterification reaction (H), the hydroxyl group of ISB can attack two different carbonyl carbon atoms in Ac-CHDA (paths a and b).

Table 2. . Comparative *Trans* Ratio of CHDA and Ac-CHDA at Various Temperature

sample code	Ac_2O (mol %)	temperature (°C)	heating time (h)	*trans* contents (monomer)
CHDA[a]	0	–	–	21.5
CHDA-180[b]	0	180	6	10.7
CHDA-200	0	200	6	27.0
CHDA-250	0	250	6	46.7
CHDA-180a1[c]	1	180	6	10.1
CHDA-200a1	1	200	6	20.0
CHDA-250a1	1	250	6	53.2
Ac-CHDA[d]	220	120	1	36.5
Ac-CHDA-180[e]	220	180	1	53.6
Ac-CHDA-200	220	200	1	60.0
Ac-CHDA-250	220	250	1	65.9

[a]CHDA: Neat CHDA. [b]CHDA-180−250: The heat treated CHDA during 6 h at 180, 200, and 250 °C, respectively. [c]CHDA-180a1−250a1: The heat treated CHDA using 1 mol % Ac_2O during 6 h at 180, 200, and 250 °C, respectively. [d]Ac-CHDA: The acetylated CHDA using 220 mol % during 1 h at 120 °C. [e]Ac-CHDA-180−250: The heat treated Ac-CHDA during 1 h at 180, 200, and 250 °C, respectively.

Scheme 5. Infinite Loop of Acetylation Using Ac_2O in the PICD Polymerization Process

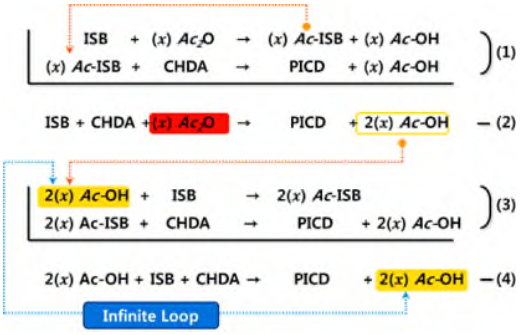

The reaction with the acetyl carbonyl carbon atom, which is far from the cyclohexane ring of Ac-CHDA (path b), may occur easily due to less steric hindrance, creating Ac-ISB (B). However, in this reaction, the AcOH byproduct of esterification with the carbonyl carbon atom adjacent to the cyclohexane ring is constantly removed from the system by acetylated free ISB and evaporation, thereby accelerating the forward reaction (path a). In this *in situ* acetylation polymerization, small amount of Ac_2O act very effectively in the acetylation and form high molecular weight polymer. If the AcOH is constantly evaporated out of reaction mixture, the concentration of Ac-ISB(B) will decrease and then the rate of polymerization will also decrease. This phenomenon might indicate the possibility of another reaction (path c) to form the Ac-ISB(B) before the AcOH is removed during the esterification (H). Free ISB(D) attacks orthoformate type intermediate (I) to develope hydrate form of ester(J) and Ac-ISB(B). Then, dehydration reaction occurrs to make PICD oligomer and H_2O.

In Table 2, although Ac-CHDA heated at 200 °C reaches a *trans* ratio of 60 mol % within 1 h, CHDA-180−250 show a much slower isomerization. In addition, both CHDA-250 and CHDA-250a1 did not reach the thermal equilibrium ratio even under identical esterification reaction conditions (temperature and time). The low *trans* ratio indicates that isomerization was not fully activated at 200 °C but proceeded rapidly as the temperature increased to 250 °C. Moreover, the *trans* ratios of CHDA-180−250 and CHDA-180a1−250a1 were similar. Because the acetylation rate of CHDA is lower than that of ISB, the acetylation of CHDA was not sufficient even after 6 h with 1 mol % Ac_2O. Under these circumstances, the epimerization of the CHDA-250a1 series cannot be activated due to the lack of an acetylation reaction. Therefore, the probability of Ac-CHDA acting as an intermediate in Scheme 4 is likely based on the *trans* ratio of oligomer made by adding just 1 mol % of Ac_2O to a PICD esterification, as shown in Table 1S, Supporting Information. In the case of PICD polymerization via *in situ* acetylation, the Ac_2O reacted preferably with ISB directly and not with CHDA (Scheme 4). In addition, AcOH, which is generated as a byproduct, could have proceeded with an acetylation reaction with free ISB. The presence of this AcOH increases the rate of polymerization and has an important effect on the whole polymerization stage.

The suggested reaction process is illustrated in Scheme 5. The x mol of Ac_2O generates $2x$ mol of AcOH via acetylation. If the AcOH is not promptly taken out of system, it can acetylate free ISB, indicating that Ac_2O acts as a catalyst in the polymerization process.

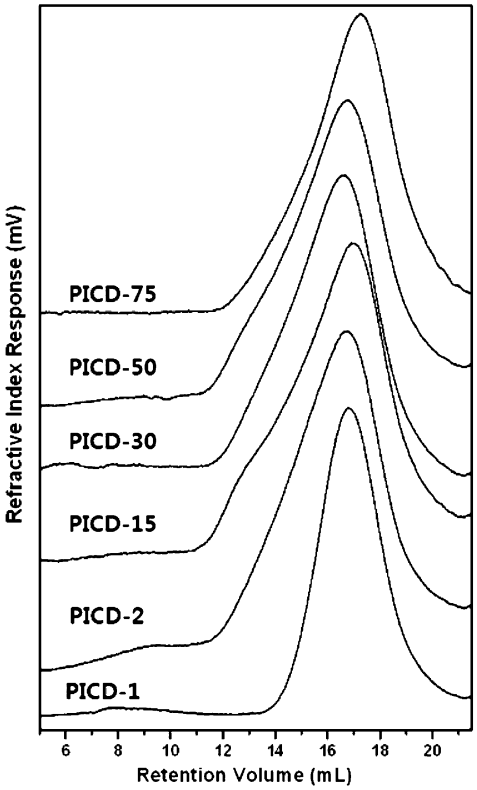

Figure 6. GPC data of PICD polymers.

Properties of PICD Homopolyester. In Figure 6, GPC chromatogram curve of PICD-1 is narrower than other samples (PICD-2−PICD-75) because of having small MWD. Generally, MWD values of polycondensated polyester are about 2−3. In the study of polycondensation of succinic acid and ISB, MWD

Scheme 6. Various Reactions Involved in the Polycondensation of PICD

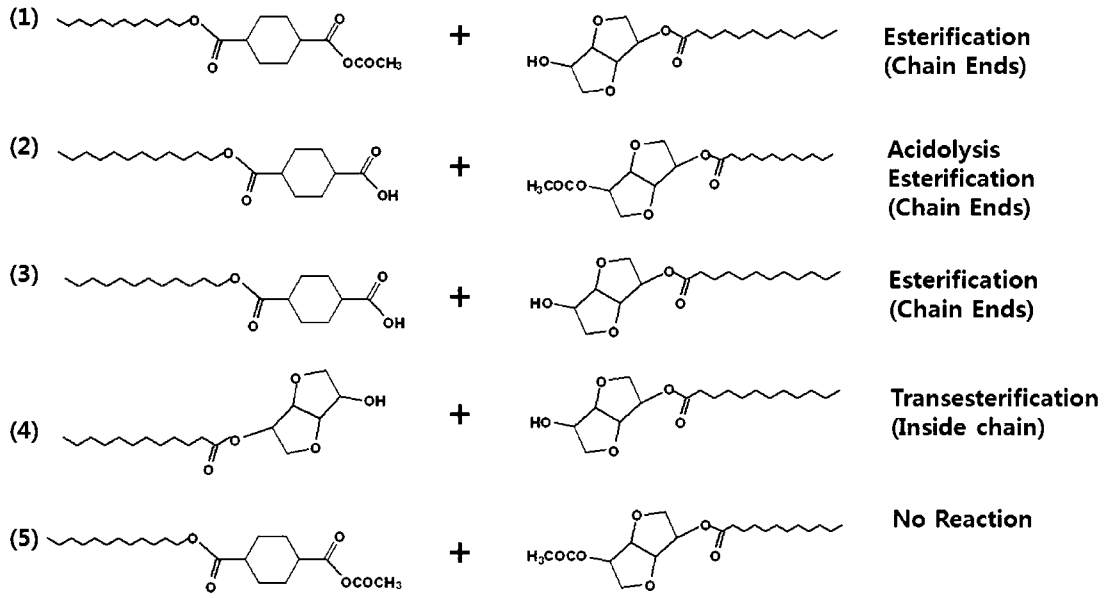

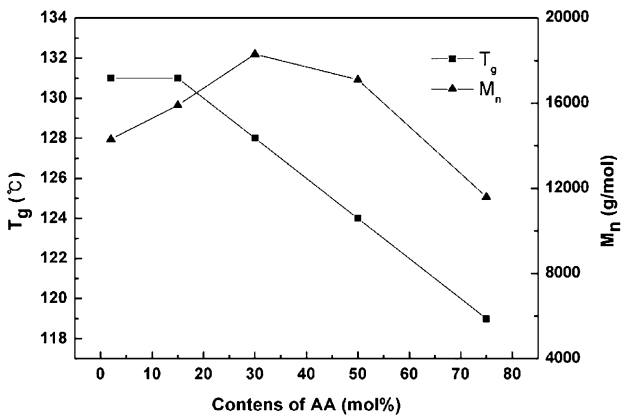

Figure 7. Variation of T_g and M_n as Ac_2O contents.

Table 3. Variation of T_g Against Open-Ring ISB and Mn

sample code	open-ring ISB (mol %)	M_n	T_g
PICD-2	3.8	14 300	131
PICD-15	5.1	15 900	131
PICD-30	14.8	18 300	128
PICD-50	28.0	17 100	124
PICD-75	21.6	11 600	119

is around 2.[17] In case of *in situ* acetylation polymerization, acidity in the system is relatively high enough to form 1,4 sorbitan (open ring structure) by breakage of ISB. This results in the formation of branch structure in the polymer chain and giving broad MWD to PICD polymer. Figure 1S (see the Supporting Information) shows the variation of the η' of PICD-1−PICD-75 at 270 °C from 0.05 rad/s to 600 rad/s. In Figure 1S (Supporting Information), PICD-2−PICD-75 which have broad MWD, shows that the onset shear rate of shear thinning is shorter compared with PICD-1. The shear viscosity at the extremely low shear rate is dependent on the M_w of each sample. Also, the hydrodynamic volume of branched polymer at low shear region in the melt state is relatively higher than that

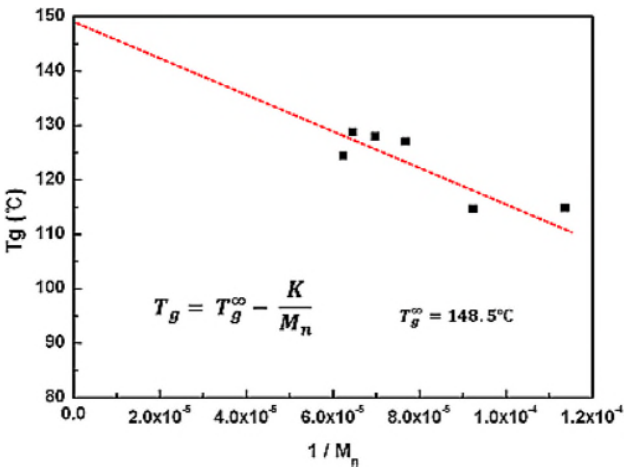

Figure 8. Infinite T_g (T_g^∞) of PICD.

of nonbranched polymer, which means that the branched polymer has higher free volume. This larger free volume enables polymer chain to be compressed at a high shear rate, leading to increase the degree of shear thinning, which is pseudoplasticity. As shown in Figure 1S (Supporting Information), the degree of shear thinning of PICD-1 is lower than that of PICD-2−PICD-75. Degrees of polymerization (M_n) of PICD-1 and PICD-75 are the same in Table 1. However, the amount of branch structure by open-ring ISB of PICD-75 is larger than PICD-1 due to higher AcOH contents in polymerization. The noticeable difference of shear-thinning between PICD-1 and PICD-75 is shown in this melt curve. This may reflect the branch structure leading to high MWD of PICD-2 to PICD-75.

The possible polycondensation of the PICD polymer is shown in reactions 1−5 in Scheme 6. Because the acetyl end group cannot attack carbonyl carbon within the polymer chain, the transesterification reaction of PICD does not occur easily. Although the end hydroxyl group of ISB attacks the carbonyl carbon atom inside chain, the rate of transesterification is slow

due to its relatively low reactivity, low volatility and large steric hindrance. For such reasons, PICD polycondensation may preferentially occur at the end group. With four possible reactions, the broad MWD can be affected by differences in the rate of chain growth between the more reactive (1) + (2) and the lesser reactive (3) + (4) reactions.

Transition temperature variations can occur from its structurally sensitive characteristics. Steric effects and intra/intermolecular interactions are two main factors, which in this case, correlates to the Ac_2O content, M_n value and amount of opened ring structure of ISB. Before explaining the data, it is important to know that ISB structure, originally rigid, changes to flexible opened ring structure. It is obvious to see that this structural change greatly affects the T_g of PICD.

In Table 1, T_g of PICD-1 is low due to the lowest Ac_2O content, resulting low molecular weight. Normally, T_g increases with the M_n until a critical value is reached. However, as shown in Figure 7. T_g and M_n shows no relation to each other. T_g tends to gradually decrease with increasing contents. (Also, Figures 2S and 3S in the Supporting Information are illustrated for more understanding.)

In Table 3, M_n, T_g and relative proportions of opened-ring structure of ISB by ^{1}H NMR peaks are compared in order of increasing Ac_2O content. PICD-2 to PICD-30 shows higher T_g due to low amount of flexible opened-ring structure of ISB and relatively high M_n. Whereas PICD-50 shows lower T_g than PICD-30 resulting from almost twice the amount of opened-ring structure of ISB, even though PICD-50 shows higher M_n. For PICD-75, M_n is lowest and the amount of opened-ring structure of ISB has high value resulting in the lowest value for T_g

According to Garaleh et al.,[43] the maximum T_g of PICD, synthesized from dichloride of CHDA and ISB, is 145 °C, which is similar to T_g^∞ calculated using the Fox and Flory equation shown below. From Doolittle's free volume theory and the WLF equation, Fox and Flory presented the relationship between T_g and M_n as eq 1.

$$T_g = T_g^\infty - \frac{K}{M_n} \tag{1}$$

In this equation, T_g^∞ is the glass transition temperature of a polymer with infinite molecular weight and K is a constant related to the thermal expansion coefficients above and below T_g. This equation shows that T_g will increase with the M_n of the polymer, leveling off at certain plateau value (T_g^∞). As shown in Figure 8, we obtained a T_g^∞ of 148.5 °C with a K of 340,062 by plotting T_g against $1/M_n$ using the data in Table 1.

■ CONCLUSIONS

Important aspects of improving polymerizations involving ISB were discussed. Ac_2O was shown to be an attractive reagent for accelerating the formation of homopolyesters with diols having low reactivity. In addition, small amounts of Ac_2O were considerably effective at increasing the molecular weight of PICD. This suggests that acetylation by Ac_2O can be used in mass production facilities. Ac_2O is easily available and the amount of AcOH byproduct, which can corrode the reactor interior, is negligible. More study is required to determine the best means of controlling and reducing anisotropic reactivity resulting from the heterogeneity of acetylation. However, the acetylation method described herein using Ac_2O was shown to increase the reactivity of other secondary alcohols and rigid glycols.

■ ASSOCIATED CONTENT

Ⓢ Supporting Information

Comparison results of trans contents of CHDA in PICD oligomer and polymer, rheological data by ARES and T_g variation graphs with M_n and open ring ISB. This material is available free of charge via the Internet at http://pubs.acs.org/.

■ AUTHOR INFORMATION

Corresponding Author

*E-mail: imss007@hanyang.ac.kr.

Notes

The authors declare no competing financial interest.

■ REFERENCES

(1) Besset, C.; Pascault, J. P.; Fleury, E.; Drockenmuller, E.; Bernard, J. *Biomacromolecules* **2010**, *11* (10), 2797−2803.
(2) Fletcher, H. G.; Goepp, R. M. *J. Am. Chem. Soc.* **1945**, *67* (6), 1042−1043.
(3) Hockett, R. C.; Fletcher, H. G.; Sheffield, E. L.; Goepp, R. M. *J. Am. Chem. Soc.* **1946**, *68* (6), 927−930.
(4) Hockett, R. C.; Sheffield, E. L. *J. Am. Chem. Soc.* **1946**, *68* (6), 937−939.
(5) Stoss, P.; Hemmer, R. *Adv. Carbohyd. Chem. Biochem.* **1991**, *49*, 93−173.
(6) Yokoe, M.; Aoi, K.; Okada, M. *J. Polym. Sci., Polym. Chem.* **2005**, *43* (17), 3909−3919.
(7) Feng, X. H.; East, A. J.; Hammond, W. B.; Zhang, Y.; Jaffe, M. *Polym. Adv. Technol.* **2011**, *22* (1), 139−150.
(8) Fenouillot, F.; Rousseau, A.; Colomines, G.; Saint-Loup, R.; Pascault, J. P. *Prog. Polym. Sci.* **2010**, *35* (5), 578−622.
(9) Habeych, D. I.; Juhl, P. B.; Pleiss, J.; Vanegas, D.; Eggink, G.; Boeriu, C. G. *J. Mol. Catal. B: Enzymol.* **2011**, *71* (1−2), 1−9.
(10) Quintana, R.; de Ilarduya, A. M.; Alla, A.; Munoz-Guerra, S. *J. Polym. Sci., Polym. Chem.* **2011**, *49* (10), 2252−2260.
(11) Majdoub, M.; Loupy, A.; Fleche, G. *Eur. Polym. J.* **1994**, *30* (12), 1431−1437.
(12) Storbeck, R.; Ballauff, M. *J. Appl. Polym. Sci.* **1996**, *59* (7), 1199−1202.
(13) Kricheldorf, H. R.; Gomourachvili, Z. *Macromol. Chem. Phys.* **1997**, *198* (10), 3149−3160.
(14) Philip, B.; Sreekumar, K. *J. Mater. Sci.* **2003**, *38* (7), 1573−1577.
(15) Chatti, S.; Bortolussi, M.; Bogdal, D.; Blais, J. C.; Loupy, A. *Eur. Polym. J.* **2004**, *40* (3), 561−577.
(16) Chatti, S.; Bortolussi, M.; Bogdal, D.; Blais, J. C.; Loupy, A. *Eur. Polym. J.* **2006**, *42* (2), 410−424.
(17) Noordover, B. A. J.; van Staalduinen, V. G.; Duchateau, R.; Koning, C. E.; van Benthem, R. A. T. M.; Mak, M.; Heise, A.; Frissen, A. E.; van Haveren, J. *Biomacromolecules* **2006**, *7* (12), 3406−3416.
(18) Kricheldorf, H. R.; Behnken, G.; Sell, M. *J. Macromol. Sci. A* **2007**, *44* (7−9), 679−684.
(19) Sablong, R.; Duchateau, R.; Koning, C. E.; de Wit, G.; van Es, D.; Koelewijn, R.; van Haveren, J. *Biomacromolecules* **2008**, *9* (11), 3090−3097.
(20) Gohil, R. M. *Polym. Eng. Sci.* **2009**, *49* (3), 544−553.
(21) Jasinska, L.; Koning, C. E. *J. Polym. Sci., Polym. Chem.* **2010**, *48* (24), 5907−5915.
(22) Bersot, J. C.; Jacquel, N.; Saint-Loup, R.; Fuertes, P.; Rousseau, A.; Pascault, J. P.; Spitz, R.; Fenouillot, F.; Monteil, V. *Macromol. Chem. Phys.* **2011**, *212* (19), 2114−2120.
(23) Tan, L. C.; Chen, Y. W.; Zhou, W. H.; Wei, J. C.; Ye, S. W. *J. Appl. Polym. Sci.* **2011**, *121* (4), 2291−2300.
(24) Quintana, R.; de Ilarduya, A. M.; Alla, A.; Guerra, S. M. *High Perform. Polym.* **2012**, *24* (1), 24−30.

(25) Beldi, M.; Medimagh, R.; Chatti, S.; Marque, S.; Prim, D.; Loupy, A.; Delolme, F. *Eur. Polym. J.* **2007**, *43* (8), 3415−3433.
(26) Lee, C. H.; Takagi, H.; Okamoto, H.; Kato, M.; Usuki, A. *J. Polym. Sci., Polym. Chem.* **2009**, *47* (22), 6025−6031.
(27) Marin, R.; Munoz-Guerra, S. *J. Appl. Polym. Sci.* **2009**, *114* (6), 3723−3736.
(28) Varkey, E. C.; Sreekumar, K. *J. Mater. Sci.* **2010**, *45* (7), 1912−1920.
(29) Marin, R.; Alla, A.; de Ilarduya, A. M.; Munoz-Guerra, S. *J. Appl. Polym. Sci.* **2012**, *123* (2), 986−994.
(30) Chrysanthos, M.; Galy, J.; Pascault, J. P. *Polymer* **2011**, *52* (16), 3611−3620.
(31) Lukaszczyk, J.; Janicki, B.; Kaczmarek, M. *Eur. Polym. J.* **2011**, *47* (8), 1601−1606.
(32) Caouthar, A. A.; Loupy, A.; Bortolussi, M.; Blais, J. C.; Dubreucq, L.; Meddour, A. *J. Polym. Sci., Polym. Chem.* **2005**, *43* (24), 6480−6491.
(33) Caouthar, A.; Roger, P.; Tessier, M.; Chatti, S.; Blais, J. C.; Bortolussi, M. *Eur. Polym. J.* **2007**, *43* (1), 220−230.
(34) Hu, J. S.; Ren, S. C.; Zhang, B. Y.; Chao, C. Y. *J. Appl. Polym. Sci.* **2008**, *109* (4), 2187−2194.
(35) Kricheldorf, H. R.; Berghahn, M.; Probst, N.; Gurau, M.; Schwarz, G. *React. Funct. Polym.* **1996**, *30* (1−3), 173−189.
(36) Lin, Q.; Pasatta, J.; Long, T. E. *J. Polym. Sci., Polym. Chem.* **2003**, *41* (16), 2512−2520.
(37) Sapich, B.; Stumpe, J.; Kricheldorf, H. R.; Fritz, A.; Schonhals, A. *Macromolecules* **2001**, *34* (16), 5694−5701.
(38) Zhang, B. Y.; Hu, J. S.; Wang, B.; Yao, D. S.; Li, H. *Colloid Polym. Sci.* **2007**, *285* (15), 1683−1690.
(39) Jackson, W. J.; Gray, T. F.; Caldwell, J. R. *J. Appl. Polym. Sci.* **1970**, *14* (3), 685−&.
(40) Chen, L. P.; Yee, A. F.; Goetz, J. M.; Schaefer, J. *Macromolecules* **1998**, *31* (16), 5371−5382.
(41) Liu, J. W.; Yee, A. F. *Macromolecules* **1998**, *31* (22), 7865−7870.
(42) Noordover, B. A. J.; Duchateau, R.; van Benthem, R. A. T. M.; Ming, W.; Koning, C. E. *Biomacromolecules* **2007**, *8* (12), 3860−3870.
(43) Garaleh, M.; Yashiro, T.; Kricheldorf, H. R.; Simon, P.; Chatti, S. *Macromol. Chem. Phys.* **2010**, *211* (11), 1206−1214.
(44) Vasquez, T. E.; Bergset, J. M.; Fierman, M. B.; Nelson, A.; Roth, J.; Khan, S. I.; O'Leary, D. J. *J. Am. Chem. Soc.* **2002**, *124* (12), 2931−2938.
(45) Zhu, Y.; Molinier, V.; Durand, M.; Lavergne, A.; Aubry, J. M. *Langmuir* **2009**, *25* (23), 13419−13425.
(46) Stoss, P.; Merrath, P.; Schluter, G. *Synthesis-Stuttgart* **1987**, *2*, 174−176.
(47) Tamion, R.; Marsais, F.; Ribereau, P.; Queguiner, G.; Abenhaim, D.; Loupy, A.; Munnier, L. *Tetrahedron-Asymm.* **1993**, *4* (8), 1879−1890.
(48) Colonna, M.; Berti, C.; Binassi, E.; Celli, A.; Fiorini, M.; Marchese, P.; Messori, M.; Brunelle, D. J. *Polym. Int.* **2011**, *60* (11), 1607−1613.